JOURNAL OF NATURAL PRODUCTS

Article

pubs.acs.org/jnp

Bioactive Anthraquinone Derivatives from the Mangrove-Derived Fungus *Stemphylium* sp. 33231

Xue-Ming Zhou,[†] Cai-Juan Zheng,[†] Guang-Ying Chen,* Xiao-Ping Song, Chang-Ri Han, Gao-Nan Li, Yan-Hui Fu, Wen-Hao Chen, and Zhi-Gang Niu

Key Laboratory of Tropical Medicinal Plant Chemistry of Ministry of Education, Hainan Normal University, Haikou 571158, People's Republic of China

Supporting Information

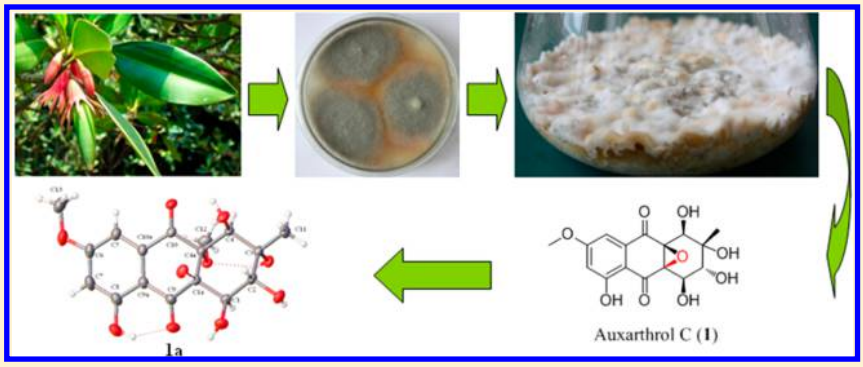

ABSTRACT: Four new anthraquinone derivatives (**1**−**4**) and four new alterporriol-type anthranoid dimers (**14**−**17**), along with 17 analogues, were isolated from the solid rice fermentation of the fungus *Stemphylium* sp. 33231 obtained from the mangrove *Bruguiera sexangula* var. *rhynchopetala* collected from the South China Sea. Their structures were elucidated using comprehensive spectroscopic methods. The absolute configurations of **1**, **3**, and **4** were determined by single-crystal X-ray diffraction of their derivatives (**1a**, **3b**, and **4a**). The absolute configurations of the chiral **17**−**19** were determined by comparing their CD spectra with **21**. The inhibitory activities of most of the compounds against seven terrestrial pathogenic bacteria and two cancer cell lines were evaluated.

Endophytic fungi are well known as rich sources of new natural products with promising biological and pharmacological activities.[1−3] Fungi in the genus *Stemphylium* produce various bioactive metabolites. Among them, the anthraquinone derivatives possess an especially wide range of biological activities.[4,5] For instance, the tetrahydroanthraquinone altersolanol A has shown cytotoxic activity against the K562 cell line,[6] while anthranoid dimer alterporriol D showed selective inhibition of bacteria.[7] In our investigation of natural antibacterial and cytotoxic products from mangrove fungi in the South China Sea, two new antibacterial α-pyrone derivatives were obtained from *Stemphylium* sp. 33231 in potato glucose liquid medium.[8] In order to search for additional bioactive natural products from *Stemphylium* sp. 33231, the culture condition was changed to a solid rice fermentation. The EtOAc extract of the fungal culture exhibited cytotoxic activity against the A549 cell lines and antibacterial activity against *Staphylococcus albus*. Bioassay-guided fractionation of the EtOAc extract led to the isolation of four new anthraquinone derivatives, auxarthrol C (**1**), macrosporin 2-*O*-(6′-acetyl)-*a*-D-glucopyranoside (**2**), 2-*O*-acetylaltersolanol B (**3**), and 2-*O*-acetylaltersolanol L (**4**), and four alterporriol-type anthranoid dimers, alterporriols T−W (**14**−**17**). Also 17 known analogues were isolated: dihydroaltersolanol A (**5**),[9] macrosporin (**6**),[10] macrosporin-7-*O*-sulfate (**7**),[11] altersolanols A−C (**8**−**10**)[9,10,12−14] and L (**11**),[15] ampelanol (**12**),[11] tetrahydroaltersolanol B (**13**),[16] and alterporriols A, B, D, and E (**18**−**21**)[14,17−19] and C, N, R, and Q (**22**−**25**).[9] Herein, we report the isolation, structure elucidation, and biological activities of these compounds.

RESULTS AND DISCUSSION

Auxarthrol C (**1**) was obtained as a white powder, with the molecular formula $C_{16}H_{16}O_9$ (nine degrees of unsaturation) from HRESIMS data combined with ^{1}H and ^{13}C NMR spectroscopic data (Tables 1 and 2). In the ^{1}H NMR spectrum one hydrogen-bonded hydroxy group at δ_H 11.14 (s), two meta-coupled aromatic hydrogens at δ_H 6.91 (d, J = 2.4 Hz) and 6.84 (d, J = 2.4 Hz), three oxygenated methine signals at δ_H 4.43 (d, J = 7.2), 4.41 (dd, J = 7.8, 6.0 Hz), and 3.27 (dd, J = 7.8, 6.6 Hz), one methoxy group at δ_H 3.88 (s), and one singlet methyl group at δ_H 1.12 (s) were observed. In the ^{13}C NMR spectrum, two carbonyl carbons (δ_C 193.4 and 191.0), six olefinic carbons (δ_C 165.2, 161.8, 134.3, 109.8, 106.8, and 105.8), six O-bearing carbons (δ_C 73.8, 71.6, 68.2, 67.4, 67.0, and 66.9), one methoxy

Received: April 16, 2014
Published: August 19, 2014

Chart 1

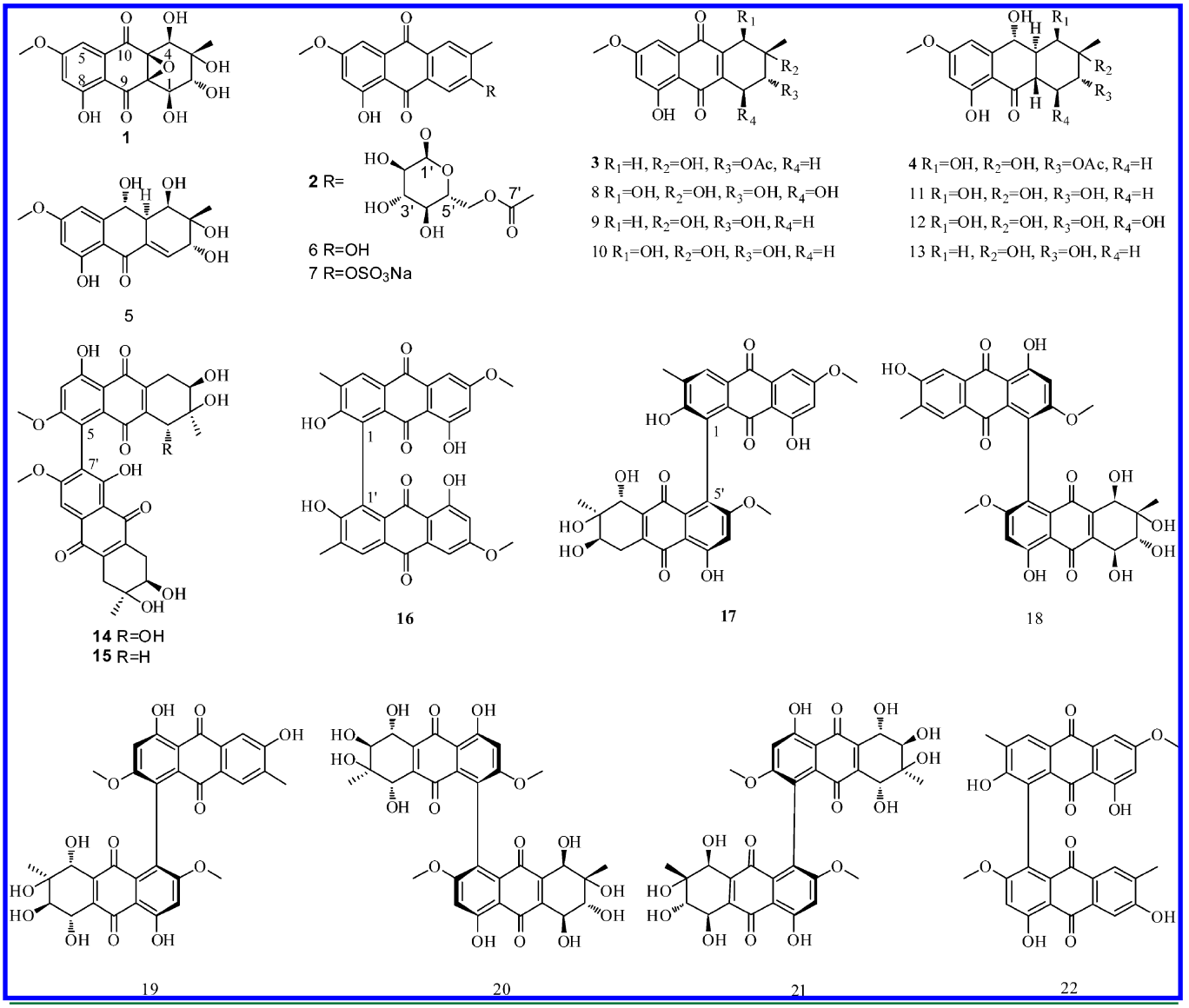

carbon (δ_C 56.2), and one methyl carbon (δ_C 21.6) were observed. These spectroscopic features suggested that **1** has a hydroanthraquinone skeleton. The ^{1}H NMR data (Table 1) were very similar to those of auxarthrol A,[20] except for the absence of a C-1 methylene signal and the presence of a hydroxy signal δ_H 5.19 (d, J = 6.0 Hz) and a methine signal δ_H 4.41 (dd, J = 7.8, 6.0 Hz) for C-1 in **1**. These data indicated that one proton on the methylene in auxarthrol A was replaced by a hydroxy in **1**. This was referred by the ^{13}C NMR spectrum (Table 2), where the C-1 signal moved downfield to δ_C 67.0 (CH) in **1** compared to δ_C 35.9 (CH_2) in auxarthrol A. The large $^3J_{H\text{-}1,\ H\text{-}2}$ = 8.4 Hz showed that H-1 and H-2 have a trans diaxial relationship. The NOESY correlation of H-2/3-Me indicated that H-2 and 3-Me should be placed on the same face. The relative configuration of the remaining stereocenters of **1** could not be firmly established due to the lack of evidence. To complete the assignment, an X-ray crystal structure was desired. However, single crystals of **1** were not obtained. To improve the crystallinity, many attempts were made to structurally modify **1**. Ultimately, opening of the epoxide with $CH_3O^-Na^+$–CH_3OH yielded **1a** (Supporting Information, Figure S67).[21] Crystallization of **1a** from CH_3OH–H_2O (10:1) resulted in colorless crystals, which gave an X-ray crystal structure with a Flack parameter of 0.02(5). Thus, the absolute configuration of **1** was determined as 1*R*,2*R*,3*R*,4*R*,1a*S*,4a*R* (Figure 1).

Compound **2** was obtained as a yellow powder, with the molecular formula $C_{24}H_{24}O_{11}$ calculated from HRESIMS data. The ^{1}H and ^{13}C NMR spectroscopic data (Tables 3 and 4) indicated that **2** was composed of one macrosporin (**6**)[10] subunit, one glucose subunit, and one acetoxy group. The location of the glucose at C-2 and the acetoxy group at C-6′ was confirmed by the HMBC correlation between H-1′ and C-2, and H-6′ and C-7′. The glycone part of **2**, a glucose moiety, was identified and characterized by the presence of six carbon signals (δ_C 97.7, 72.9, 71.3, 71.1, 70.0, 63.3) and a signal for one anomeric proton doublet at δ_H 5.71 (J = 3.6 Hz; H-6′), respectively. The large $^3J_{H\text{-}2',\ H\text{-}3'}$ = 9.2 Hz, $^3J_{H\text{-}3',\ H\text{-}4'}$ = 9.6 Hz, and $^3J_{H\text{-}4',\ H\text{-}5'}$ = 9.6 Hz revealed the axial–axial relationship for these protons. These data suggested that the glycosyl moiety was α-glucose. Acid hydrolysis of **2** produced glucose as the sole sugar identified on the basis of TLC by comparing with an authentic sugar sample. The glucose isolated from the hydrolysate gave a positive optical rotation, $[\alpha]^{24}_D$ +45 (c 0.2, H_2O), and indicated that it is D-glucose. Therefore, the glycosyl moiety was an

dx.doi.org/10.1021/np500340y | J. Nat. Prod. 2014, 77, 2021–2028

Table 1. ^{1}H NMR Data for 1 (600 MHz), 3, 4, and 16 (400 MHz) (δ in ppm, J in Hz)

position	1[a]	3[b]	4[a]	16[b]
1	4.41, dd (7.8, 6.0)	2.79, dd (19.2, 7.6 H-1ax)	1.59, dd (12.4, 12.0 H-1ax)	
		3.04, dd (19.2, 5.6 H-1eq)	2.11, ddd (12.4, 4.8, 4.0 H-1eq)	
2	3.27, dd (7.8, 6.6)	5.00, dd (7.6, 5.6)	4.90 dd (12.0, 4.8)	
4	4.43, d (7.2)	2.68, d (19.2 H-4ax)	3.84, d (2.4)	8.16, br s
		2.91, d (19.2 H-4eq)		
5	6.91, d (2.4)	7.14, d (2.4)	6.76, dd (2.4, 1.2)	7.24, d (2.4)
7	6.84, d (2.4)	6.60, d (2.4)	6.34, d (2.4)	6.64, d (2.4)
10			4.66, dd (10.8, 6.8)	
1a			2.76, ddd (12.4, 12.0, 4.0)	
4a			2.25, ddd (12.4, 10.8, 2.4)	
12		2.14, s	2.05, s	
3-Me	1.12, s	1.34, s	1.15, s	2.43, s
6-OMe	3.88, s	3.89, s	3.82, s	3.95, s
1-OH	5.19, d (6.0)			
2-OH	4.66, d (6.6)			
3-OH	4.55, s		4.57, s	
4-OH	5.50, d (7.2)		5.29, d (6.0)	
8-OH	11.14, s	12.21, s	12.86, s	12.63, s
10-OH			5.67, d (6.8)	

[a]DMSO-d_6. [b]Acetone-d_6.

Table 2. ^{13}C NMR Data for 1 (125 MHz), 3, 4, and 16 (100 MHz) (δ in ppm)

position	1[a]	3[b]	4[a]	16[b]
1	67.0, CH	26.6, CH_2	26.0, CH_2	128.5, C
2	71.6, CH	73.7, CH	73.5, CH	159.9, C
3	68.2, C	69.5, C	71.3, C	125.5, C
4	66.9, CH	36.1, CH_2	72.3, CH	131.1, CH
5	106.8, CH	108.0, CH	104.3, CH	107.4, CH
6	165.2, C	166.0, C	165.9, C	167.0, C
7	105.8, CH	106.1, CH	99.0, CH	106.6, CH
8	161.8, C	164.3, C	164.5, C	166.2, C
9	193.4, C	187.3, C	203.6, C	189.2, C
10	191.0, C	183.4, C	66.0, CH	182.1, C
1a	67.4, C	141.4, C	41.2, CH	133.0, C
4a	73.8, C	142.1, C	45.7, CH	132.1, C
9a	109.8, C	109.5, C	108.9, C	111.8, C
10a	134.3, C	133.6, C	152.0, C	135.9, C
11		170.6, C	170.3, C	
12		21.2, CH_3	21.0, CH_3	
3-Me	21.6, CH_3	25.6, CH_3	23.1, CH_3	17.3, CH_3
6-OMe	56.2, CH_3	56.1, CH_3	55.7, CH_3	56.6, CH_3

[a]DMSO-d_6. [b]Acetone-d_6.

α-D-glucopyranoside, and the absolute configuration of **2** is as shown.

2-*O*-Acetylaltersolanol B (**3**) was obtained as an orange-yellow powder. Its molecular formula of $C_{18}H_{18}O_7$ (10 degrees of unsaturation) was determined by HRESIMS. The molecular formula was also corroborated by ^{1}H and ^{13}C NMR spectroscopic data (Tables 1 and 2). Its ^{1}H and ^{13}C NMR spectra closely resembled those of altersolanol B (**9**)[9] except for the presence of one acetoxy signal (δ_C 170.6, 21.2 and δ_H 2.14, s) in **3**. The location of the acetoxy group at C-2 was confirmed by the HMBC correlation between H-2 and C-11. In the NOESY spectrum 3-Me showed a correlation to H-2, indicating that 3-Me and H-2 should be placed on the same face. To assign the absolute configuration of **3**, a hydrolysis reaction was adopted for **3** to obtain **3a**. Furthermore, altersolanol B 2,3-*O*-acetonide (**3b**) was prepared from **3a** according to a previously reported method.[18] Finally, an X-ray crystal structure of **3b** with a Flack parameter of 0.02(11) was obtained (Figure 2). Ultimately, the absolute configuration of **3** was established as 2*R*,3*S*.

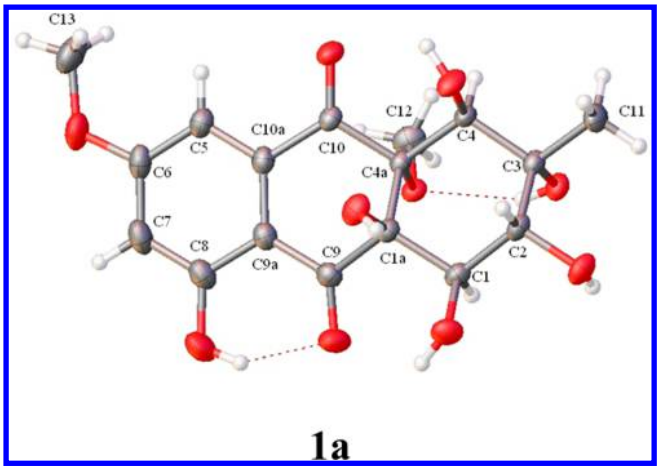

Figure 1. X-ray structure of **1a**.

2-*O*-Acetylaltersolanol L (**4**) was obtained as a white powder. Its molecular formula of $C_{18}H_{22}O_8$ (eight degrees of unsaturation) was determined by HRESIMS. Careful comparison of the ^{1}H NMR and ^{13}C NMR spectra of **4** (Tables 1 and 2) with those of altersolanol L (**11**)[15] showed a close structural relationship except for the presence of an acetoxy group (δ_C 170.3, 21.0 and δ_H 2.05, s) in **4**. The location of the acetoxy group at C-2 was established by the HMBC correlation between H-2 and C-11. The large $^3J_{H\text{-}10,\ H\text{-}4a}$ = 10.8 Hz and $^3J_{H\text{-}4a,\ H\text{-}1a}$ = 12.4 Hz showed that H-10 and H-4a/H-4a and H-1a have trans diaxial relationships, which was corroborated by the correlations of H-1a with H-10 and H-2 and H-2 with 3-Me in the NOESY spectrum. To assign the full relative and absolute configuration of **4**, a hydrolysis reaction was adopted for **4** to obtain **4a** (Figure S69).[9] Crystallization of **4a** from CH_3OH–$CHCl_3$ (1:1) resulted in colorless crystals, which gave an X-ray crystal structure with a Flack parameter of −0.03(15). Thus, the absolute configuration of **4** was established as 2*R*,3*S*,4*R*,1a*S*,4a*S*,10*R* (Figure 3).

Alterporriol T (**14**) was obtained as an orange, amorphous powder, with the molecular formula $C_{32}H_{30}O_{13}$ from HRESIMS data. The ^{1}H and ^{13}C NMR spectroscopic data (Tables 3 and 4) indicated that **14** was comprised one altersolanol C (**10**)[9] subunit and one altersolanol B (**9**)[9] subunit. In the ^{1}H NMR spectrum of **14**, two aromatic proton signals were assigned to H-7 in the altersolanol C moiety at δ_H 6.87 (s) and to H-5′ in the altersolanol B moiety at δ_H 7.27 (s). In anthranoid dimer systems the two meta-coupled aromatic protons H-5 (H-5′) and H-7 (H-7′) differ considerably with regard to their chemical shifts, with H-5 (H-5′) consistently resonating more downfield (~7.2 ppm) than H-7 (H-7′, ~6.8 ppm).[22] This observation proved vital to assign the position of the intersubunit linkage in **14**. Therefore, **14** was lacking a proton signal at C-5 in the aromatic altersolanol C moiety and at C-7′ in the altersolanol B moiety. Furthermore, the HMBC spectrum showed that H-7 correlated to C-6 and C-8, while H-5′ correlated to C-7′

dx.doi.org/10.1021/np500340y | J. Nat. Prod. 2014, 77, 2021−2028

Table 3. ^{1}H NMR Data for 2, 14, 15, and 17 (400 MHz) (δ in ppm)

position	2[a]	14[b]	15[b]	17[a]	17[c]
1	7.87, s	2.53, dd (19.2, 9.2 H-1ax) 2.98, dd (19.2, 6.0 H-1eq)	2.73−2.90, m		
2		3.94, m	3.80, dd (5.6, 5.2)		
4	8.01, br s	4.38, d (6.0)	2.68, dd (19.2, 3.2) 2.76, dd (19.2, 2.4)	7.88, br s	8.10, d (0.4)
5	7.18, d (2.8)			7.11, d (2.8)	7.26, d (2.8)
7	6.86, d (2.8)	6.87, s	6.86, s	6.64, d (2.8)	6.63, d (2.8)
3-Me	2.39, br s	1.39, s	1.22, s	2.10, s	3.91, s
6-OMe	3.93, s	3.84, s	3.84, s	3.88, s	2.34, d (0.4)
4-OH		4.43, d (6.0)			
1′	5.71, d (3.6)	2.73−2.90, m	2.73−2.90, m	2.34, dd (19.2, 9.6 H-1ax) 2.72, dd (19.2, 6.0 H-1eq)	2.51, dd (19.2, 9.6 H-1ax) 3.00, dd (19.2, 6.0 H-1eq)
2′	3.51 m	3.83, m	3.76, dd (5.6, 5.6)	3.69, dd (9.6, 6.0)	3.88, dd (9.6, 6.0)
3′	3.69, ddd (9.6, 9.2, 5.2)				
4′	3.23 m	2.69, d (18.8) 2.78, d (18.8)	2.41, d (19.2) 2.58, d (19.2)	4.10, s	4.29, s
5′	3.61, ddd (9.6, 6.4, 2.4)	7.27, s	7.29, s		
6′	4.10, dd (12.0, 6.4 H-6′ ax) 4.16 dd (12.0, 2.4 H-6′ eq)			6.80, s	6.88, s
7′					
8′	1.85, s				
3′-Me		1.31, s	1.31, s	1.16, s	1.34, s
6′-OMe		3.83, s	3.84, s	3.65, s	3.74, s
8-OH	12.75, s	13.06, s	13.11, s	13.03, s	
1′-OH					
2′-OH	5.35, d (3.6)			4.69, br s	
3′-OH	5.21, d (5.2)			4.36, br s	
4′-OH	5.33, d (6.4)			5.56, br s	
8′-OH		12.28, s	12.27, s	12.82, s	

[a]DMSO-d_6. [b]Acetone-d_6. [c]CD_3OD.

and C-10′. These results indicated that the two monomers were joined via a C-5−C-7′ linkage. Thus, alterporriol T (**14**) was identified as a new anthranoid dimer with a C-5 and C-7′ linkage. Due to the biosynthetic pathway, the configuration of **14** was tentatively assigned as 2*R*,3*R*,4*R*,2′*R*,3′*S*,[10] but the absolute configurations for the axes of chirality in **14** have not been determined.

Alterporriol U (**15**) was also obtained as an orange, amorphous powder. Its molecular formula, $C_{32}H_{30}O_{12}$ (18 degrees of unsaturation), was obtained from HRESIMS data. The ^{1}H and ^{13}C NMR (Tables 3 and 4) spectroscopic data indicated that **15** comprised two altersolanol B (**9**)[9] units, but it is not a symmetrical dimer. In the ^{1}H NMR spectrum, two aromatic protons at δ_H 6.86 (s) and 7.29 (s) were observed. These results indicated that the two monomers were also joined via a C-5−C-7′ linkage as in **14**. This was corroborated by the HMBC spectrum (H-7 correlated with C-6 and C-8, and H-5′ correlated with C-7′ and C-10′). Thus, **15** was identified as a new anthranoid dimer with a C-5 and C-7′ linkage. Due to the biosynthetic pathway, the configuration of **15** was also tentatively assigned as 2*R*,3*S*,2′*R*,3′*S*.[10] However, the absolute configurations for the axes of chirality in **15** have not been determined.

Alterporriol V (**16**) was obtained as a yellow, amorphous powder, with the molecular formula $C_{32}H_{22}O_{10}$ from HRESIMS data. However, there were only 16 signals present in the ^{13}C NMR spectrum. This result indicated that compound **16** was a symmetrical dimer. Careful comparison of the ^{1}H NMR and ^{13}C NMR spectra of **16** (Tables 1 and 2) with those of macrosporin (**6**)[10] showed a close structural relationship except for the absence of the aromatic proton at δ_H 7.52 (H-1) in **16** and the fact that the chemical shift of C-1 moved significantly downfield (δ_C 128.5, C in **16** vs 111.0, CH in **2**). These data confirmed that compound **16** was a symmetrical dimer of **2** with a C-1 and C-1′ linkage. Thus, alterporriol V (**16**) was identified as a new symmetrical dimer with a C-1 and C-1′ linkage, but the absolute configurations for the axes of chirality in **16** have not been determined.

Alterporriol W (**17**) was obtained as a red, amorphous powder with the molecular formula $C_{32}H_{26}O_{12}$ from HRESIMS data. The ^{1}H and ^{13}C NMR spectroscopic data (Tables 3 and 4) indicated that **17** was composed of one altersolanol C (**10**)[9] subunit and one macrosporin (**6**)[10] subunit. In the ^{1}H NMR spectrum, four aromatic proton signals were observed, among which three were due to C-4, C-5, and C-7 in the macrosporin moiety at δ_H 7.88 (br s), 7.11 (d, J = 2.8 Hz), and 6.64 (d, J = 2.8 Hz) and one due to C-7′ in the altersolanol C moiety at δ_H 6.80 (s). Therefore, **17** lacked proton signals corresponding to C-1 in **6** and to C-5′ in **10**. These results indicated that the two monomers were joined via a C-1−C-5′ linkage. The configuration of **17** also has been tentatively assigned as 2′*R*,3′*R*,4′*R*.[10]

An interesting feature of the isolated anthranoid dimers is their axial chirality. CD spectra of **18**/**19** and **20**/**21** recorded in MeOH showed a near-quasi-mirror images pattern (Figure 4). This is due to the chiral axis occurring within the chromophore, and it is expected to dominate the observed CD spectrum.[22,23] So, these CD spectra indicated that they (**18** and **19**, **20** and **21**)

dx.doi.org/10.1021/np500340y | J. Nat. Prod. 2014, 77, 2021−2028

Table 4. ^{13}C NMR Data for 3, 14, 15, and 17 (100 MHz) (δ in ppm)

position	2[a]	14[b]	15[b]	17[a]
1	110.8, CH	29.6, CH_2	30.3, CH_2	131.0, C
2	159.8, C	68.7, CH	71.9, CH	164.2, C
3	135.0, C	73.4, C	70.6, C	131.0, C
4	129.6, CH	70.9, CH	36.3, CH_2	129.3, CH
5	107.3, CH	117.5, C	117.6, C	105.5, CH
6	166.0, C	165.8, C	165.8, C	165.3, C
7	106.0, CH	104.5, CH	104.5, CH	104.8, CH
8	164.6, C	165.5, C	165.2, C	163.2, C
9	186.2, C	189.8, C	189.6, C	189.3, C
10	180.8, C	184.8, C	184.5, C	178.5, C
1a	133.0, C	142.6, C	142.5, C	130.6, C
4a	127.0, C	144.6, C	143.9, C	125.6, C
9a	110.2, C	110.4, C	110.2, C	110.5, C
10a	134.8, C	133.5, C	131.8, C	136.0, C
3-Me	16.3, CH_3	22.3, CH_3	25.4, CH_3	56.4, CH_3
6-OMe	56.4, CH_3	57.1, CH_3	57.1, CH_3	17.6, CH_3
1′	97.7, CH	30.3, CH_2	30.6, CH_2	28.8, CH_2
2′	71.3, CH	71.9, CH	71.8, CH	67.0, CH
3′	72.9, CH	70.6, C	70.5, C	72.0, C
4′	70.0, CH	36.1, CH_2	36.1, CH_2	69.1, CH
5′	71.1, CH	103.4, CH	103.3, CH	125.5, C
6′	63.3, CH_2	163.6, C	163.8, C	164.6, C
7′	170.1, C	120.1, C	120.1, C	102.8, CH
8′	20.4, CH_3	161.7, C	161.4, C	163.2, C
9′		190.1, C	189.9, C	188.5, C
10′		184.3, C	184.3, C	183.6, C
1a′		143.8, C	141.9, C	141.5, C
4a′		144.6, C	144.5, C	144.5, C
9a′		110.8, C	110.8, C	108.8, C
10a′		133.5, C	133.5, C	131.8, C
3′-Me		25.5, CH_3	25.5, CH_3	21.9, CH_3
6′-OMe		56.8, CH_3	56.8, CH_3	56.0, CH_3

[a]DMSO-d_6. [b]Acetone-d_6.

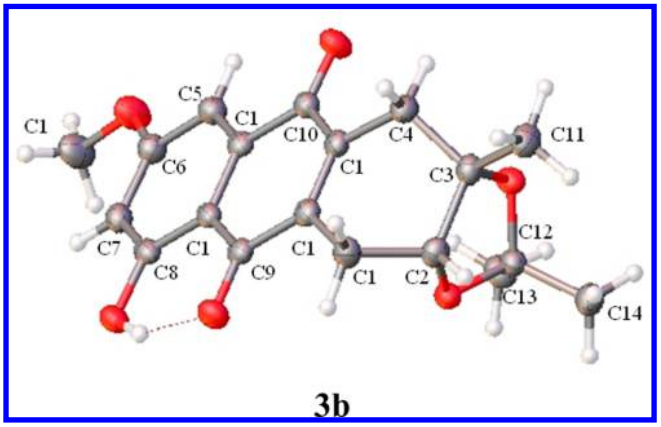

Figure 2. X-ray structure of 3b.

have different axial chiralities. However, the axial chiralities of 18 and 19 have not yet been assigned. In order to assign axial chiralities of 17−19, their CD spectra were compared with known compound 21. Regarding their biaryl chromophoric system, 17 and 19 showed the same spectral feature in the 205−340 nm range as 21 (Figure 5) and their CD are primarily determined by their axial chirality, so they must have the same a*R* axial chirality, whereas 18 has an a*S* configuration.[7,18] Thus, the

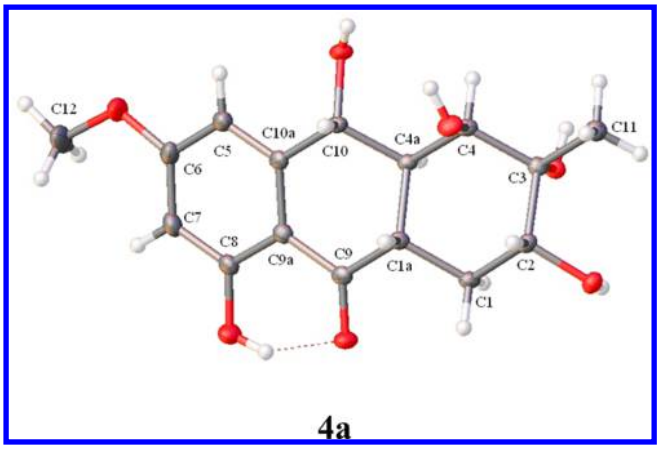

Figure 3. X-ray structure of 4a.

overall absolute configuration of 17 has been tentatively assigned as a*R*,2′*R*,3′*R*,4′*S*.

Another interesting phenomenon of 18 and 19 is their crystallization. When they were in a 1:1 mixture, it was easy to crystallize. However, it was difficult to obtain a single crystal when they were separated. Ultimately, the absolute configurations of 18 and 19 were confirmed by mixed crystal X-ray crystallography (Figure S66). Thus, the absolute configurations of 18 and 19 have been assigned as a*S*,1′*S*,2′*R*,3′*S*,4′*R* and a*R*,1′*S*,2′*R*,3′*S*,4′*R*, respectively.

The structures of known compounds 5−13 and 18−25 were identified by comparison of their $^1H/^{13}C$ NMR spectra and $[\alpha]^{24}_D$ with those in the literature.

Compounds 1−9, 11, 15−22, and 25 were evaluated for cytotoxic activities against the mouse melanoma cell line (B16F10) and the human lung adenocarcinoma cell line (A549). However, in the assay all IC_{50} values obtained were higher than 10 μM and were defined as inactive.

The antibacterial activities of all compounds were determined against seven terrestrial pathogenic bacteria: *Micrococcus tetragenus*, *Escherichia coli*, *Staphylococcus albus*, *Bacillus cereus*, *S. aureus*, *Kocuria rhizophila*, and *Bacillus subtilis* (Table 5). Compounds 3, 8, and 9 exhibited only weak broad-spectrum antibacterial activities against *E. coli*, *S. aureus*, and *B. subtilis*, while 8 exhibited weak antibacterial activity against *S. aureus* with an MIC value 2.07 μM. These results indicated that anthraquinone derivatives showed better antibacterial activities than anthraquinone dimers in these assays. All compounds were tested for brine shrimp lethality using *Artemia salina* (brine shrimp).[24] Only compound 2 displayed a moderate lethality effect, with an LD_{50} value of 10 μM.

EXPERIMENTAL SECTION

General Experimental Procedures. Optical rotations were measured on a JASCO P-1020 digital polarimeter. UV spectra were recorded on a Beckman DU 640 spectrophotometer. CD spectra were recorded on a MOS-450 spectrometer. IR spectra were recorded on a Nicolet 6700 spectrophotometer. NMR spectra were recorded on a Bruker AV spectrometer (400 MHz for ^1H and 100 MHz for ^{13}C) and a JEOL JEM-ECP NMR spectrometer (600 MHz for ^1H and 150 MHz for ^{13}C). TMS was used as an internal standard. HRESIMS spectra were measured on a Q-TOF Ultima Global GAA076 LC mass spectrometer. Silica gel (Qing Dao Hai Yang Chemical Group Co.; 200−300 mesh), octadecylsilyl silica gel (YMC; 12 nm−50 μm), and Sephadex LH-20 (GE) were used for column chromatography (CC). Precoated silica gel plates (Yan Tai Zi Fu Chemical Group Co.; G60, F-254) were used for

dx.doi.org/10.1021/np500340y | J. Nat. Prod. 2014, 77, 2021−2028

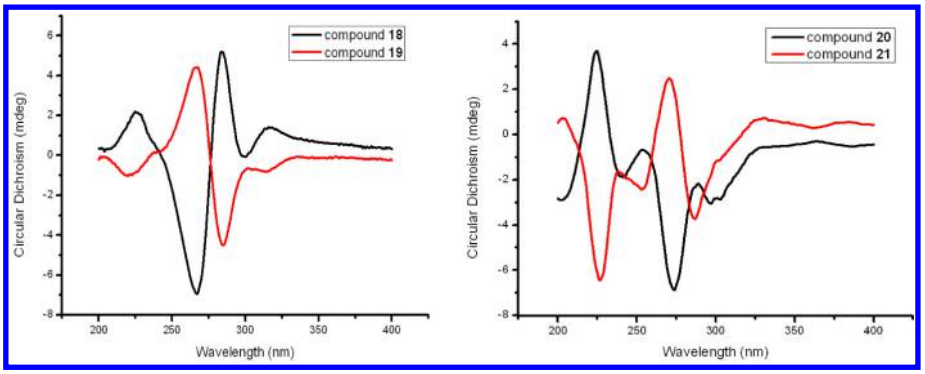

Figure 4. CD spectra of **18**, **19**, **20** and **21**.

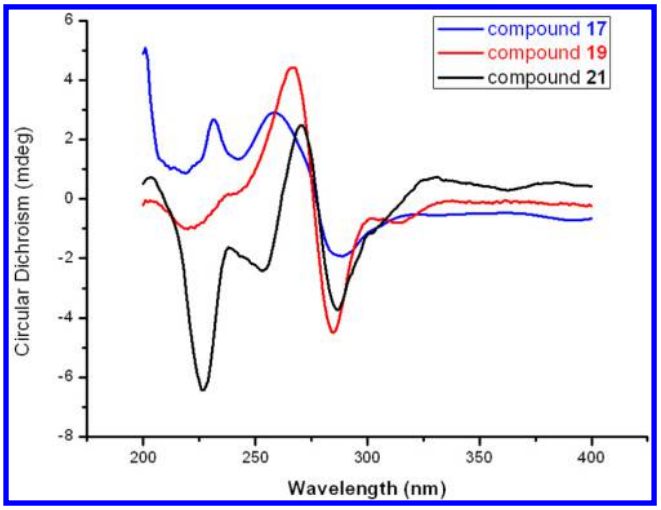

Figure 5. CD spectra of **17**, **19** and **21**.

thin-layer chromatography (TLC). X-ray diffraction data were collected on an Aglient Technologies Gemini A Ultra system.

Fungal Materials. The fungal strain *Stemphylium* sp. 33231 was isolated from the mangrove *Burguiera sexangula* var. *rhynchopetala* collected in the South China Sea in August 2012.[8] The strain was deposited in the Key Laboratory of Tropical Medicinal Plant Chemistry of Ministry of Education, College of Chemistry and Chemical Engineering, Hainan Normal University, P. R. China, with a GenBank accession number KF479349.

Fermentation, Extraction, and Isolation. The fungal strain was grown on solid rice cultures in 1 L Erlenmeyer flasks (276 flasks; 100 mL of natural seawater from the South China Sea was added to 100 g of commercially available rice, autoclave sterilization) at 25 °C without shaking for 4 weeks. The fermentation was extracted three times with an equal volume of EtOAc. The combined EtOAc layers were evaporated to dryness under reduced pressure to give an EtOAc extract (225.4 g), which was subjected to silica gel CC (petroleum ether, EtOAc, MeOH v/v, gradient) to generate nine fractions (Frs. 1–9). Fr. 2 was isolated by CC on silica gel eluting with petroleum ether–EtOAc (5:1) to obtain **6** (5.8 g). Fr. 4 was isolated by CC on silica gel eluting with petroleum ether–EtOAc (1:1) and then subjected to repeated Sephadex LH-20 CC eluting with mixtures of $CHCl_3$–MeOH (1:1) to obtain **9** (25 mg), **10** (15.2 mg), **16** (8.8 mg), **22** (5.5 mg), and **25** (7.5 mg). Fr. 5 was isolated by CC on silica gel eluting with $CHCl_3$–MeOH (35:1) and then subjected to Sephadex LH-20 CC eluting with $CHCl_3$–MeOH (1:1) and further purified by using octadecylsilyl silica gel eluting with 40% MeOH–H_2O to obtain **8** (28.5 mg), **4** (12.5 mg) **13** (43.5 mg), **14** (18.2 mg), **15** (8.7 mg), and **17** (6.3 mg). Fr. 6 was isolated by CC on silica gel eluting with $CHCl_3$–MeOH (25:1) and then subjected to Sephadex LH-20 CC eluting with $CHCl_3$–MeOH (1:1) and further purified by using octadecylsilyl silica gel eluting with 45% MeOH–H_2O to obtain **1** (13.9 mg), **3** (48.8 mg), **5** (9.2 mg), **8** (5.7 mg), **11** (10.6 mg), and **23** (12.5 mg). Fr. 7 was isolated by CC on silica gel eluting with $CHCl_3$–MeOH (15:1) and then subjected to Sephadex LH-20 CC eluting with $CHCl_3$–MeOH (1:1) and further purified by using

Table 5. Antimicrobial Activities of Isolated Compounds[a]

	MIC (μM)						
compound	*M. tetragenus*	*E. coli*	*S. albus*	*B. cereus*	*S. aureus*	*K. rhizophila*	*B. subtilis*
1	>10	9.8	>10	>10	>10	>10	>10
3	7.8	3.9	3.9	>10	3.9	>10	3.9
6	4.6	4.6	>10	>10	9.2	>10	>10
8	8.2	4.1	>10	>10	2.07	>10	4.1
9	>10	7.8	>10	>10	7.8	7.8	7.8
10	>10	>10	>10	>10	>10	>10	8.8
13	>10	7.3	>10	>10	>10	>10	>10
15	>10	>10	>10	8.3	>10	>10	>10
16	>10	>10	>10	8.1	>10	>10	>10
19	>10	>10	>10	7.9	>10	>10	>10
20	>10	7.5	>10	10.0	5.0	>10	>10
21	>10	5.0	>10	2.50	>10	>10	>10
22	>10	>10	8.9	>10	>10	>10	>10
ciprofloxacin[b]	0.3	0.3	0.6	0.6	0.16	0.3	0.6

[a]Compounds **2**, **4**, **5**, **7**, **11**, **12**, **14**, **17**, **18**, and **23**–**25** are inactive for all terrestrial pathogenic bacteria used (MIC > 10 μM/L). [b]Ciprofloxacin was used as a positive control.

dx.doi.org/10.1021/np500340y | *J. Nat. Prod.* 2014, 77, 2021–2028

octadecylsilyl silica gel eluting with 50% MeOH−H_2O to obtain **2** (3.8 mg), **18** (11.2 mg), and **19** (8.7 mg). Fr. 8 was isolated by CC on silica gel eluting with $CHCl_3$−MeOH (9:1) and then subjected to Sephadex LH-20 CC eluting with $CHCl_3$−MeOH (1:1) and further purified by using octadecylsilyl silica gel eluting with 50% MeOH−H_2O to obtain **7** (88.7 mg), **24** (6.1 mg), **21** (5.4 mg), and **20** (10.5 mg) respectively.

Auxarthrol C (**1**): white powder; $[\alpha]^{24}_D$ −160 (*c* 0.4, MeOH); UV (MeOH) λ_{max} (log ε) 358 (0.85), 310 (0.98), and 249 (2.29) nm; IR (KBr) ν_{max} 3421, 3011, and 1722 cm^{-1}; ^1H and ^{13}C NMR, see Tables 1 and 2; HRESIMS *m*/*z* 351.0711 $[M - H]^-$ (calcd for $C_{16}H_{15}O_9$, 351.0716).

Macrosporin 2-O-(6′-acetyl)-a-D-glucopyranoside (**2**): yellow powder; $[\alpha]^{24}_D$ +120 (*c* 0.3, MeOH); UV (MeOH) λ_{max} (log ε) 310 (1.41), 281 (4.21), and 219 (2.50) nm; IR (KBr) ν_{max} 3498, 1692, 1633, and 1573 cm^{-1}; ^1H and ^{13}C NMR, see Tables 3 and 4; HRESIMS *m*/*z* 487.1238 $[M - H]^-$ (calcd for $C_{24}H_{23}O_{11}$, 487.1240).

2-O-Acetylaltersolanol B (**3**): orange-yellow powder; $[\alpha]^{24}_D$ −85.7 (*c* 0.25, MeOH); UV (MeOH) λ_{max} (log ε) 427 (0.89) and 258 (3.11) nm; IR (KBr) ν_{max} 3440, 1643, and 1019 cm^{-1}; ^1H and ^{13}C NMR, see Tables 1 and 2; HRESIMS *m*/*z* 345.0971 $[M - H]^-$ (calcd for $C_{18}H_{17}O_7$, 345.0974).

2-O-Acetylaltersolanol L (**4**): white powder; $[\alpha]^{24}_D$ −48.8 (*c* 0.35, MeOH); UV (MeOH) λ_{max} (log ε) 316 (1.98), 261 (3.29), and 242 (2.02) nm; IR (KBr) ν_{max} 3438, 1638, and 1391 cm^{-1}; ^1H and ^{13}C NMR, see Tables 1 and 2; HRESIMS *m*/*z* 367.1391 $[M + H]^+$ (calcd for $C_{18}H_{23}O_8$, 367.1393).

Alterporriol T (**14**): orange, amorphous powder; $[\alpha]^{24}_D$ +64 (*c* 0.2, MeOH); UV (MeOH) λ_{max} (log ε) 438 (0.80), 271 (2.63), and 239 (1.47) nm; CD (*c* 1.61 × 10^{-1} mol/L, MeOH) λ_{max} ($\Delta\varepsilon$) 337 (5.08), 271 (−1.49), and 214 (1.35); IR (KBr) ν_{max} 3441, 1637, and 1398 cm^{-1}; ^1H and ^{13}C NMR, see Tables 3 and 4; HRESIMS *m*/*z* 621.1603 $[M - H]^-$ (calcd for $C_{32}H_{29}O_{13}$, 621.1608).

Alterporriol U (**15**): orange, amorphous powder; $[\alpha]^{24}_D$ −200 (*c* 0.3, MeOH); UV (MeOH) λ_{max} (log ε) 438 (1.46) and 255 (3.93) nm; CD (*c* 1.65 × 10^{-1} mol/L, MeOH) λ_{max} ($\Delta\varepsilon$) 327 (−6.78), 265 (0.09), and 212 (−1.52); IR (KBr) ν_{max} 3435, 2971, 1644, and 1397 cm^{-1}; ^1H and ^{13}C NMR, see Tables 3 and 4; HRESIMS *m*/*z* 605.1653 $[M - H]^-$ (calcd for $C_{32}H_{29}O_{12}$, 605.1659).

Alterporriol V (**16**): yellow, amorphous powder; $[\alpha]^{24}_D$ −186 (*c* 0.15, MeOH); UV (MeOH) λ_{max} (log ε) 401 (0.49), 287 (1.81), and 237 (0.95) nm; IR (KBr) ν_{max} 3424, 2923, 1630, 1572, and 1304 cm^{-1}; ^1H and ^{13}C NMR, see Tables 1 and 2; HRESIMS *m*/*z* 565.1133 $[M - H]^-$ (calcd for $C_{32}H_{21}O_{10}$, 565.1135).

Alterporriol W (**17**): red, amorphous power; $[\alpha]^{24}_D$ +198 (*c* 0.15, MeOH); UV (MeOH) λ_{max} (log ε) 338 (1.50), 229 (4.29), and 207 (1.89) nm; CD (*c* 1.66 × 10^{-1} mol/L, MeOH) λ_{max} ($\Delta\varepsilon$) 289 (−1.93), 258 (2.90), and 232 (2.65); IR (KBr) ν_{max} 3440 and 1610 cm^{-1}; ^1H and ^{13}C NMR, see Tables 3 and 4; HRESIMS *m*/*z* 601.1342 $[M - H]^-$ (calcd for $C_{32}H_{25}O_{12}$, 601.1346).

Alterporriol A (**18**): CD (*c* 1.62 × 10^{-1} mol/L, MeOH) λ_{max} ($\Delta\varepsilon$) 316 (1.42), 284 (5.21), 267 (−6.96), and 225 (2.19).

Alterporriol B (**19**): CD (*c* 1.58 × 10^{-1} mol/L, MeOH) λ_{max} ($\Delta\varepsilon$) 314 (−0.81), 285 (−4.50), 266 (4.40), and 220 (−1.02).

X-ray Crystal Structure Analysis of Compounds 1a, 3b, and 4a and Mixed Crystal of 18 and 19. Crystal X-ray diffraction data were collected on a Bruker APEX DUO diffractometer with Cu Kα radiation (λ = 1.5418 and 1.541 84 Å). The structure was solved by direct methods (SHELXS-97) and refined using full-matrix least-squares difference Fourier techniques. Carbon and oxygen atoms were refined anisotropically. Hydrogen atoms were either refined freely with isotropic displacement parameters or positioned with an idealized geometry and refined riding on their parent C atoms. Crystals suitable for X-ray diffraction (**1a** and **3b**) were obtained by slow evaporation of a solution in MeOH−H_2O, and **4a** was obtained by slow evaporation of a solution in MeOH−$CHCl_3$. The mixed crystal of **18** and **19** was obtained by slow evaporation of a solution in MeOH−DMSO. Crystallographic data (excluding structure factors) for **1a**, **3b**, and **4a** and the mixed crystal of **18** and **19** have been deposited with the Cambridge Crystallographic Data Centre: CCDC reference numbers 972307, 979866, 972306, and 979867. These data can be obtained, free of charge, from the Cambridge Crystallographic Data Centre via http://www.ccdc.cam.ac.uk/data_request/cif.

Crystal data for **1a**: $C_{17}H_{20}O_{10}$, *M* = 384.33, space group $P2_12_12_1$ with *a* = 6.1647(7) Å, *b* = 11.40078(15) Å, *c* = 23.0795(3) Å, $\alpha = \beta = \gamma = 90°$, *V* = 1622.09(4) $Å^3$, *Z* = 4, *T* = 293(2) K, D_c = 1.574 g/cm^3, μ(Cu Kα) = 1.130 mm^{-1}, *F*(000) = 808, 8631 reflections measured, 2807 independent reflections (R_{int} = 0.0219). The final R_1 values were 0.0265 [$I > 2\sigma(I)$]. The final wR_2 (F^2) values were 0.0653 [$I > 2\sigma(I)$]. The final R_1 values were 0.0283 (all data). The final wR_2 (F^2) values were 0.0672 (all data). Flack parameter = 0.02(5).

Crystal data for **3b**: $C_{19}H_{20}O_6$, *M* = 344.35, space group $P2_12_12_1$ with *a* = 7.97730(10) Å, *b* = 20.0228(3) Å, *c* = 20.8545(3) Å, $\alpha = \beta = \gamma = 90°$, *V* = 3331.05(8) $Å^3$, *Z* = 8, *T* = 119.99(18) K, D_c = 1.373 g/cm^3, μ(Cu Kα) = 0.851 mm^{-1}, *F*(000) = 1456, 20 601 reflections measured, 5564 independent reflections (R_{int} = 0.0362). The final R_1 values were 0.0303 [$I > 2\sigma(I)$]. The final wR_2 (F^2) values were 0.0704 [$I > 2\sigma(I)$]. The final R_1 values were 0.0335 (all data). The final wR_2 (F^2) values were 0.0725 (all data). Flack parameter = 0.02(11).

Crystal data for **4a**: $C_{16}H_{20}O_7$, *M* = 324.32, space group $P2_12_12_1$ with *a* = 5.66941(19) Å, *b* = 10.8760(4) Å, *c* = 23.9077(7) Å, $\alpha = \beta = \gamma = 90°$, *V* = 1474.16(8) $Å^3$, *Z* = 4, *T* = 110.02(10) K, D_c = 1.461 g/cm^3, μ(Cu Kα) = 0.971 mm^{-1}, *F*(000) = 688, 6945 reflections measured, 2514 independent reflections (R_{int} = 0.0286). The final R_1 values were 0.0313 [$I > 2\sigma(I)$]. The final wR_2 (F^2) values were 0.0765 [$I > 2\sigma(I)$]. The final R_1 values were 0.0330 (all data). The final wR_2 (F^2) values were 0.0779 (all data). Flack parameter = −0.03(15).

Crystal data for mixed crystal of **18** *and* **19**: $3(C_2H_6OS)\cdot 2(C_{32}H_{26}O_{13})\cdot 6(O)$, *M* = 1567.44, space group P_1 with *a* = 9.18695(15) Å, *b* = 9.48126(17) Å, *c* = 21.1713(3) Å, α = 82.3800(14)°, β = 83.5029(13)°, γ = 79.8305(14)°, *V* = 1791.47(5) $Å^3$, *Z* = 1, *T* = 120.0(2) K, D_c = 1.453 g/cm^3, μ(Cu Kα) = 1.780 mm^{-1}, *F*(000) = 818, 12 348 reflections measured, 11 844 independent reflections (R_{int} = 0.0377). The final R_1 values were 0.0496 [$I > 2\sigma(I)$]. The final wR_2 (F^2) values were 0.1394 [$I > 2\sigma(I)$]. The final R_1 values were 0.0531 (all data). The final wR_2 (F^2) values were 0.1451 (all data). Flack parameter = 0.010(9).

Biological Assays. Cytotoxic activity was evaluated by the MTT method as described previously.[25] Two cancer cell lines, the mouse melanoma cell line B16F10 and the human lung adenocarcinoma cell line A549, were used. Epirubicin was used as a positive control. Antibacterial activity was determined by the conventional broth dilution assay.[26] Seven terrestrial pathogenic bacteria, *M. tetragenus* (ATCC 13623), *E. coli* (ATCC 25922), *S. albus* (ATCC 8799), *B. cereus* (ATCC 14579), *S. aureus* (ATCC 6538), *K. rhizophila* (ATCC 9341), and *B. subtilis* (ATCC 6633), were used, and ciprofloxacin was used as a positive control. Brine shrimp toxicity of the isolated compounds was determined as described previously. Colchicine was used as a positive control.[24]

■ ASSOCIATED CONTENT

Ⓢ Supporting Information

^1H, ^{13}C, DEPT, HMQC, HMBC, COSY, NOESY, and HRESIMS spectra of the new compounds (**1**−**4**, **14**−**17**); CIF files and X-ray crystallographic data for **1a**, **3b**, **4a**, and mixed crystal of **18** and **19**. This material is available free of charge via the Internet at http://pubs.acs.org.

■ AUTHOR INFORMATION

Corresponding Author

*Tel: 86-89865889422. Fax: 86-89865889422. E-mail: chgying123@163.com.

Author Contributions

†X.-M. Zhou and C.-J. Zheng are co-first authors.

Notes

The authors declare no competing financial interest.

■ ACKNOWLEDGMENTS

This work was supported by the National Natural Science Foundation of China (21162009, 31360069) and The Major Technology Project of Hainan (ZDZX2013008-4).

■ REFERENCES

(1) Aly, A. H.; Debbab, A.; Kjer, J.; Proksch, P. *Fungal Diversity* **2010**, *41*, 1−16.
(2) Aly, A. H.; Debbab, A.; Proksch, P. *Appl. Microbiol. Biotechnol.* **2011**, *90*, 1829−1845.
(3) Debbab, A.; Aly, A. H.; Lin, W. H.; Proksch, P. *Microbiol. Biotechnol.* **2010**, *3*, 544−563.
(4) Haraguchi, H.; Abo, T.; Fukuda, A.; Okamura, N.; Yagi, A. *Phytochemistry* **1996**, *43*, 989−992.
(5) Phuwapraisirisan, P.; Rangsan, J.; Siripong, P.; Tip-Pyang, S. *Nat. Prod. Rep.* **2009**, *23*, 1063−1071.
(6) Teiten, M. H.; Mack, F.; Debbab, A.; Aly, A. H.; Dicato, M.; Proksch, P.; Diederich, M. *Bioorg. Med. Chem.* **2013**, *21*, 3850−3858.
(7) Debbab, A.; Aly, A. H.; Edrada-Ebel, R.; Wray, V.; Pretsch, A.; Pescitelli, G.; Kurtan, T.; Proksch, P. *Eur. J. Org. Chem.* **2012**, *7*, 1351−1359.
(8) Zhou, X. M.; Zheng, C. J.; Song, X. P.; Han, C. R.; Chen, W. H.; Chen, G. Y. *J. Antibiot.* **2014**, *67*, 401−403.
(9) Zheng, C. J.; Shao, C. L.; Guo, Z. Y.; Chen, J. F.; Deng, D. S.; Yang, K. L.; Chen, Y. Y.; Fu, X. M.; She, Z. G.; Lin, Y. C.; Wang, C. Y. *J. Nat. Prod.* **2012**, *75*, 189−197.
(10) Becker, A. M.; Rickards, R. W.; Schmalzl, K. J.; Yick, H. C. *J. Antibiot.* **1978**, *31*, 324−329.
(11) Aly, A. H.; Edrada-Ebel, R.; Wray, V.; Müller, W. E.; Kozytska, S.; Hentschel, U.; Proksch, P.; Ebel, R. *Phytochemistry* **2008**, *69*, 1716−1725.
(12) Stoessl, A. *Can. J. Chem.* **1969**, *47*, 767−776.
(13) Stoessl, A.; Unwin, C. H.; Stothers, J. B. *Can. J. Chem.* **1983**, *61*, 372−377.
(14) Stoessl, A. *Can. J. Chem.* **1969**, *47*, 777−784.
(15) Debbab, A.; Aly, A. H.; Edrada-Ebel, R.; Wray, V.; Müller, W. E. G.; Totzke, F.; Zirrgiebel, U.; Schächtele, C.; Kubbutat, M. H. G.; Lin, W. H.; et al. *J. Nat. Prod.* **2009**, *72*, 626−631.
(16) Stoessl, A.; Stothers, J. B. *Can. J. Chem.* **1983**, *61*, 378−382.
(17) Suemitsu, R.; Sakurai, Y.; Nakachi, K.; Miyoshi, I.; Kubota, M. *Agric. Biol. Chem.* **1989**, *53*, 1301−1304.
(18) Kanamaru, S.; Honma, M.; Murakami, T.; Tsushima, T.; Kudo, S.; Tanaka, K.; Nihei, K.; Nehira, T.; Hashimoto, M. *Chirality* **2012**, *24*, 137−146.
(19) Suemitsu, R.; Yamamoto, T.; Miyai, T.; Ueshima, T. *Phytochemistry* **1987**, *26*, 3221−3224.
(20) Alvi, K. A.; Rabenstein, J. *J. Ind. Microbiol. Biotechnol.* **2004**, *31*, 11−15.
(21) Kuniaki, T.; Yoshikazu, S.; Tatsuya, T.; Yoshiaki, F.; Seijiro, H. *Tetrahedron Lett.* **2011**, *22*, 138−148.
(22) Bringmann, G.; Menche, D.; Kraus, J.; Mühlbacher, J.; Peters, K.; Peters, E. M.; Brun, R.; Bezabih, M.; Abegaz, B. M. *J. Org. Chem.* **2002**, *67*, 5595−5610.
(23) Bringmann, G.; Mortimer, J. P. A.; Keller, P. A.; Gresser, M. J.; Garner, J.; Breuning, M. *Angew. Chem., Int. Ed.* **2005**, *44*, 5384−5427.
(24) Solis, P. N.; Wright, C. W.; Anderson, M. M. *Planta Med.* **1993**, *59*, 250−252.
(25) Scudiero, D. A.; Shoemaker, R. H.; Paull, K. D.; Monks, A.; Tierney, S.; Nofziger, T. H.; Currens, M. J.; Seniff, D.; Boyd, M. R. *Cancer Res.* **1988**, *48*, 4827−4833.
(26) Appendio, G.; Gibbons, S.; Giana, A.; Pagani, A.; Grassi, G.; Stavri, M.; Smith, E.; Rahman, M. M. *J. Nat. Prod.* **2008**, *71*, 1427−1430.

■ NOTE ADDED AFTER ASAP PUBLICATION

This paper was published on the Web on August 19, 2014, with errors in Figures 4 and 5. The corrected version was reposted on August 21, 2014.